IL-1β Epitope Mapping Using Site-Directed Mutagenesis and Hydrogen−Deuterium Exchange Mass Spectrometry Analysis

Jirong Lu,*,‡ Derrick R. Witcher,‡ Melissa A. White,‡ Xiliang Wang,§ Lihua Huang,|| Radhakrishnan Rathnachalam,⊥ John M. Beals,‡ and Stuart Kuhstoss‡

Biotechnology Discovery Research, Integrative Biology, Biopharmaceutical Research and Development, Structural Computation, Lilly Research Laboratories, Eli Lilly and Company, Indianapolis, Indiana 46285

Received March 24, 2005; Revised Manuscript Received June 7, 2005

ABSTRACT: Hu007, a humanized IgG1 monoclonal antibody, binds and neutralizes human, cynomolgus, and rabbit IL-1β but only weakly binds to mouse and rat IL-1β. Biacore experiments demonstrated that Hu007 and the type-I IL-1 receptor competed for binding to IL-1β. Increasing salt concentrations decrease the association rate with only moderate effects on the dissociation rate, suggesting that long-range electrostatics are critical for formation of the initial complex. To understand the ligand-binding specificity of Hu007, we have mapped the critical residues involved in the recognition of IL-1β. Selected residues in cynomolgus IL-1β were mutated to the corresponding residues in mouse IL-1β, and the effects of the changes on binding were evaluated by surface plasmon resonance measurements using Biacore. Specifically, substitution of F150S decreased binding affinity by 100-fold, suggesting the importance of hydrophobic interactions in stabilizing the antibody/antigen complex. Substitution of three amino acids near the N- and C-terminal regions of cIL-1β with those found in mouse IL-1β (V3I/S5Q/F150S) decreased the binding affinity of Hu007 to IL-1β by about 1000-fold. Conversely, mutating the corresponding residues in mouse IL-1β to the human sequence resulted in an increase in binding affinity of about 1000-fold. Hydrogen−deuterium exchange/mass spectrometry analysis confirmed that these regions of IL-1β were protected from exchange because of antibody binding. The results from this study demonstrate that Hu007 binds to a region located in the open end of the β-barrel structure of IL-1β and blocks binding of IL-1β to its receptor.

Interleukin-1β (IL-1β)[1] is a prototypical proinflammatory cytokine, which belongs to a family of structurally related cytokines important in health and disease. It shares a common set of receptors with two structurally related molecules, the proinflammatory cytokine IL-1α and the anti-inflammatory cytokine, IL-1 receptor antagonist (IL-1ra). IL-1α and IL-1β bind to the type-I receptor (IL-1RI) and induce signaling in concert with the IL-1 receptor accessory protein (IL-1RAcP) (*1*−*5*). The type-II receptor (IL-1RII) is a decoy receptor (*6*, *7*), which lacks a cytoplasmic signaling domain. Both IL-1RI and IL-1RII are shed from the cell surface and bind IL-1 in circulation, thus inhibiting IL-1 signaling (*8*). IL-1ra binds to both receptors without inducing signaling and therefore functions as a natural antagonist for IL-1α/β activity (*9*). The multiple levels of regulation of IL-1 activity suggest that misregulation of this important family of cytokines could lead to disease. In fact, excessive levels of IL-1β have been associated with a range of acute and chronic diseases such as sepsis and rheumatoid arthritis. In clinical trials, blockade of IL-1 activity with IL-1ra (Anakinra) has shown efficacy in rheumatoid arthritis patients (*10*, *11*). Antagonist antibodies against IL-1β could offer advantages such as increased half-life and improved efficacy in the treatment of these diseases.

Hu007 is a humanized immunoglobulin type 1 (IgG_1) monoclonal antibody that binds to and neutralizes the activity of IL-1β. Hu007 displays high-affinity binding to human, cynomolgus, and rabbit IL-1β. It binds very weakly to mouse and rat IL-1β and exhibits no detectable binding to human IL-1α or IL-1ra, which share a common β-barrel structure with IL-1β (*12*−*17*). Moreover, Hu007 does not recognize a linear epitope, because denaturation of IL-1β results in a loss of binding. Receptor-binding studies indicate that binding of Hu007 to IL-1β blocks binding of IL-1β to its receptor. To help understand this antibody-binding specificity, we have mapped the critical residues involved in recognition of IL-1β by Hu007 using a combination of site-directed mutagenesis and hydrogen−deuterium exchange mass spectrometry (H/DXMS) approaches.

Sequence alignment of IL-1β species variants identified 11 residues that were candidates for determining Hu007 specificity. The crystal structure of human IL-1β (*12*, *13*) and a homology model for cynomolgus IL-1β (cIL-1β)

* To whom correspondence should be addressed. E-mail: Lu_Jirong@lilly.com. Telephone: 317-276-4356. Fax: 317-277-8200.
‡ Biotechnology Discovery Research.
§ Integrative Biology.
|| Biopharmaceutical Research and Development.
⊥ Structural Computation.

[1] Abbreviations: H/DXMS, hydrogen−deuterium exchange mass spectrometry; H/D, hydrogen/deuterium; MS, mass spectrometry; Q-TOF, quadruple time-of-flight; CD, circular dichroism; RU, response unit; CDR, complementarity-determining region; IgG1, immunoglobulin type I; IL, interleukin; cIL-1β, cynomolgus IL-1β; IL-1RI, IL-1 type-I receptor; IL-1RII, IL-1 type-II receptor; IL-1ra, IL-1 receptor antagonist; IL-1RacP, interleukin-1 receptor accessory protein.

10.1021/bi0505464 CCC: $30.25
Published on Web 07/28/2005

showed that all 11 residues were surface-exposed. Selected residues in cIL-1β were mutated to the corresponding residues in mouse IL-1β, and the effects on binding were evaluated by Biacore analysis. To further map the binding surface, H/DXMS analysis was used and identified three regions on IL-1β that were protected from exchange upon antibody binding. Together these data support a model in which Hu007 binds to regions located on the open side of the β barrel of IL-1β and recognizes a discontinuous epitope with determinants near both the N and C termini. Residues critical to binding were further verified by converting selected residues in mouse IL-1β to the corresponding residues in human and cIL-1β and monitoring the impact on binding. Thus, by taking multiple orthogonal approaches, we were able to unambiguously identify residues critical for Hu007 binding to IL-1β.

MATERIALS AND METHODS

Materials. IL-1RI and rat IL-1β were purchased from R&D. Hu007 is a recombinant product of Eli Lilly and Company. Protein A was purchased from Calbiochem (La Jolla, CA). Reagents for Biacore experiments were purchased from Biacore AB (Uppsala, Sweden).

Construction, Mutagenesis, and Expression of IL-1β. Mature forms of human, mouse, and cynomolgus IL-1β were cloned into pET30a(+) (Novagen). Native proteins were expressed with or without a C-terminal 6× His tag to evaluate the effect of the tag on Hu007 binding. Mutant forms of protein were expressed with a 6× His tag for ease of purification. Expression was performed on *Escherichia coli* BL21 (DE3) (Novagen). Overnight cultures were subcultured into 2× TY medium containing 50 μg/mL kanamycin. Cells were grown at 37 °C, induced with 1 mM IPTG, and shaken for 4−5 h at 37 °C. Cell pellets were stored at −20 °C until purification. Mutagenesis was performed using standard PCR-based methods. Primers with appropriate coding mutations were used to generate altered molecules, and PCR products were cloned into PCR-Blunt II-TOPO (Invitrogen). Mutations I3V and Q5S in cynomolgus IL-1β were generated using a Quikchange multisite-directed mutagenesis kit (Stratagene) directly in the pET30a-(+) vector. All clones were sequence-confirmed.

Purification of Histidine-Tagged IL-1β Analogues. Concentrated media containing the IL-1β analogue (containing a 6× His tag) were placed over IMAC (immobilized metal-affinity resin, Pharmacia) 5−20 mL column at a flow rate of 2 mL/min. The column was washed with PBS (1 mM potassium phosphate, 3 mM sodium phosphate, and 0.15 M NaCl at pH 7.4) until the absorbance returned to baseline, and the bound polypeptides were eluted with a 0.050−0.5 M linear imidazol gradient (in PBS) over 60 min. Fractions containing IL-1β analogue were pooled and concentrated to 2 mL using an Ultrafree centrifugal filter unit (Millipore, 10-kDa molecular weight cutoff). This material was further purified with a Superdex 75 (Pharmacia, 16/60) sizing column equilibrated with PBS plus 0.5 M NaCl at a flow rate of 1 mL/min. Fractions containing the IL-1β analogue were analyzed by SDS−PAGE. The N-terminal sequence of the purified IL-1β analogue was confirmed (data not shown).

Purification of Untagged Human, Cynomolgus, Rabbit, and Mouse IL-1β. E. coli from 0.5 L of culture induced with IPTG were resuspended in 200 mL of a buffer containing 50 mM Tris/HCl at pH 8.5, 2 mg of lysozyme, and 80 μg of DNase and stirred for 30 min at room temperature. The mixture was sonicated for 8 min and centrifuged at 4 °C (15000*g*) for 15 min to remove the cell debris. The supernatant was loaded onto a 30 mL Q-Sepharose (Pharmacia) column at a flow rate of 3.0 mL/min, which was equilibrated with 50 mM Tris/HCl at pH 8.5 and 25 mM NaCl. The flow through of this column (which contained IL-1β) was subjected to a 50% ammonium sulfate cut for 30 min at 4 °C to remove other proteins. The supernatant from this procedure was treated with 95% ammonium sulfate for 30 min at 4 °C and centrifuged at 4000*g* for 30 min to precipitate IL-1β. The pellets were resuspended in 25 mL of 15 mM sodium phosphate at pH 5.7 and dialyzed against the same buffer. Any insoluble protein was removed by centrifugation at 4000*g* for 30 min.

The supernatant from the dialysate was loaded onto a 125 mL CM-Sepharose (Pharmacia) column equilibrated with 50 mM Tris/HCl at pH 8.5 and 25 mM NaCl at a flow rate of 3 mL/min. The column was washed until the absorbance returned to the baseline, and the bound polypeptides were eluted with a linear gradient from 25 mM to 1.0 M NaCl over 110 min. Fractions containing IL-1β were analyzed by SDS−PAGE, pooled, concentrated using an Ultrafree centrifugal filter unit (Millipore, 10-kDa molecular weight cutoff), and dialyzed against PBS. The IL-1β protein was then filtered with a Millex-GV 0.22-μm filter unit, and the N-terminal sequence was confirmed.

Far- and Near-UV Circular Dichroism (CD) Spectra of IL-1β Analogues. CD data were collected on an AVIV model 62DS spectrometer. Near-UV CD spectra were collected in a 1 cm path-length cell from 350 to 250 nm at a 1 nm bandwidth, 0.5 nm steps, and 5 s time constant. Far-UV CD spectra were collected from 260 nm to the lowest wavelength possible according to solvent conditions with a 1 nm bandwidth, 0.5 nm steps, 3 s time constant, and an appropriate cell path length to yield a sufficient signal. Both near- and far-UV CD data were blank-corrected and averaged over three spectra. Raw data was normalized by conversion to mean residue ellipticity (MRE, deg cm^2 dmol^{-1}) for structural comparison of different IL-1β analogues.

Determination of Binding Affinity and Kinetics Using Surface Plasmon Resonance. Binding affinity and kinetics of the IL-1β analogues were measured using surface plasmon resonance with a Biacore 2000 instrument containing a CM5 sensor chip. Protein A was immobilized onto flow cells 1 and 2 using amine-coupling chemistry. Flow cells were activated for 7 min with a 1:1 mixture of 0.1 M *N*-hydroxysuccinimide and 0.1 M 3-(*N*,*N*-dimethylamino)-propyl-*N*-ethylcarbodiimide at a flow rate of 5 μL/min. Protein A (35 μg/mL in 10 mM sodium acetate at pH 4.5) was injected over both flow cells for 2−3 min at 5 μL/min, which resulted in a surface density of 700−800 response units (RU). Surfaces were blocked with a 7 min injection of 1 M ethanolamine-HCl at pH 8.5. To ensure complete removal of any noncovalently bound protein A, 15 μL of 10 mM glycine at pH 1.5 was injected twice. Unless stated otherwise in the text, the running buffer used for kinetic experiments contained 10 mM HEPES at pH 7.4, 150 mM NaCl, 0.005% P20, and 3 mM EDTA, (HBS-EP) purchased from Biacore. All experiments were performed at 25 °C with

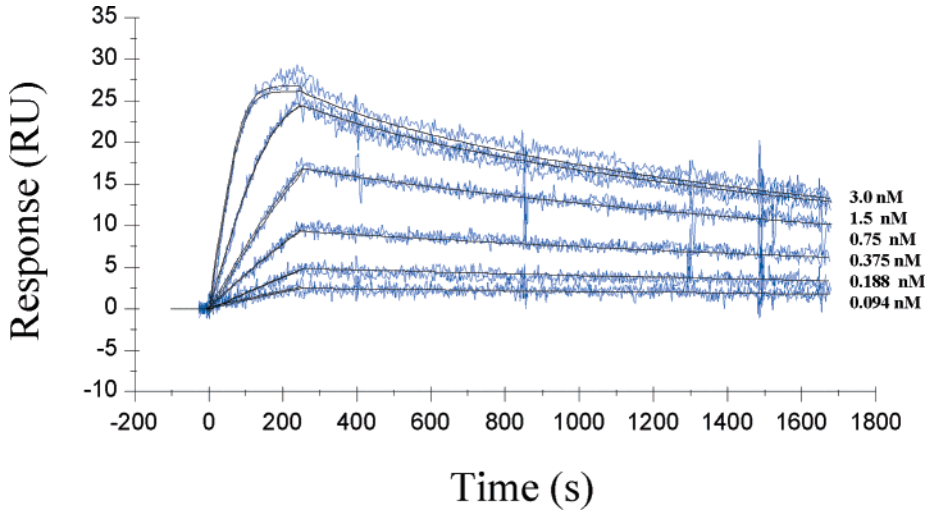

FIGURE 1: Sensorgram data and global analysis of human IL-1β binding to Hu007. IL-1β (3.0, 1.5, 0.75, 0.375, 0.188, and 0.094 nM) was injected over a control surface (no Hu007) and a surface containing ~150 RU of Hu007 with the dissociation monitored for 20 min. The data were collected in duplicate for each IL-1β concentration. The association and dissociation phases were globally fit to a 1:1 mass transport limited model. The fit of the data is shown as a solid line.

a flow rate of 60 μL/min. Each analysis cycle consisted of (i) the capture of 140−180 RU antibody by injection of 15−20 μL of approximately 2 μg/mL antibody over flow cell 2, (ii) a 2 min stabilization time, (iii) a 250 μL injection of IL-1β analogues (concentration range of 3−0.094 nM in 2-fold dilution increments) over flow cells 1 and 2, using flow cell 1 as the reference flow cell, (iv) a 20 min dissociation (buffer flow), and (v) the regeneration of protein A surface with a 1 min injection of 10 mM glycine at pH 1.5. The signal was monitored as flow cell 2 minus flow cell 1. Samples and a buffer blank were injected in duplicate. The data from buffer blank (0 nM concentration) was subtracted from all of the sample runs. This method is referred to as double referencing, which should correct for any dissociation of Hu007 from protein A during the run; however, it should be noted that during the time scale of the binding experiments no dissociation of Hu007 from protein A was observed. The normalized data were then simultaneously fit to a 1:1 binding with mass transport model using global data analysis in BIAevaluation 3.1 software to obtain k_{on} and k_{off} parameters.

H/DXMS Analysis. IL-1β and the IL-1β/Hu007 complex were prepared as follows: 20 μg of IL-1β (40 μL) solution was transferred to a 10-kD cutoff Microcon. Then, either 0 or 150 μg of Hu007 was added, yielding an approximate molar ratio of 1:1. A total of 100 μL of PBS was added into each Microcon, which was then centrifuged at 14000*g* for 10 min. This step was repeated one more time by addition of 100 μL of PBS. The protein solution (20−30 μL) was collected. A total of 6 μL of free IL-1β or the IL-1β/Hu007 complex was mixed with 14 μL of 100% D_2O, resulting in 70% D_2O in the final sample. The solution was incubated at ambient temperature for 10 min. The exchange was quenched, and the sample was digested by adding 15 μL of 0.67 mg/mL pepsin and 0.33% formic acid solution and incubating at ambient temperature for 30 s. The digest was immediately injected onto a C18 reversed-phase column, manually.

A Waters 2695 HPLC and Micromass Q-TOF micro were used for all analyses. The HPLC stream from the HPLC pump was connected to metal tubing (about 1 mL), to the manual injector, to a Zorbax C18 column (2.1 × 50 mm) and then to the mass spectrometer. The metal tubing, injector loop, and column were continuously submerged in ice water. The column was equilibrated with 98% A (0.15% formic acid aqueous solution) and 2% B (0.12% formic acid in acetonitrile) at a flow rate of 0.2 mL/min. A gradient elution was performed from 2 to 20% B over 0.5 min, to 40% B over 9.5 min, to 90% B over 1 min with 1 min hold and then rapidly returned to the initial conditions. The mass spectrometry was performed on a Micromass Q-TOF micro with the following settings: a capillary voltage of 3.0 kV, a cone voltage of 30 V, a collision energy of 10 eV, a mass range of 300 to 2000, a desolvation temperature of 250 °C, and a desolvation gas flow of 300 L/h. The mass spectrum of each peptic peptide of IL-1β was obtained after D/H exchange with or without Hu007. The average mass of each peptide was calculated according to the isotopic distribution of the most intense ion peak.

RESULTS

Binding Affinity of Hu007 to Human IL-1β—Effect of Salt Concentration. Hu007 was captured on the surface of a Biacore chip through immobilized protein A. Binding of human IL-1β to the antibody was monitored as a function of IL-1β concentrations (3.0, 1.5, 0.75, 0.375, 0.188, and 0.094 nM). Data were globally fit with 1:1 mass transport limited model to obtain k_{on} and k_{off}. Figure 1 shows an overlay of the fitted curves and data for repeated injections of six IL-1β concentrations. To investigate whether electrostatic interactions play an important role in binding of Hu007 to IL-1β, we monitored the binding as a function of the salt concentration. Under physiological salt conditions (150 mM NaCl), Hu007 binds to human IL-1β with a K_d of approximately 18 pM, with a k_{on} of 6×10^7 M^{-1} s^{-1} and a k_{off} of 11.6×10^{-4} s^{-1} (Table 1). It should be noted that similar results were obtained using a solution-based method, KinExA (data not shown). This interaction is highly dependent on the salt concentration, with an approximately 34-fold decrease in binding affinity observed when the salt concentration is raised from 150 mM to 1 M NaCl, suggesting an

Table 1: Effect of the Salt Concentration on Binding Kinetics and Affinity of Hu007 to Human IL-1β Measured by Biacore[a]

[salt] (M)	K_d (pM)	k_{on} (10^7) (M^{-1} s^{-1})	k_{off} (10^{-4}) (s^{-1})
0.15	18 ± 1	6 ± 3	11.6 ± 0.6
0.3	44 ± 4	1.42 ± 0.07	12.6 ± 0.6
0.5	111 ± 1	0.84 ± 0.01	9.4 ± 0.2
1.0	600 ± 200	0.5 ± 0.2	26 ± 4

[a] Biacore experiments were performed at 25 °C in 10 mM sodium citrate, 10 mM sodium phosphate, 3 mM EDTA, and 0.005% polysorbate-20 at pH 7.4 with NaCl concentrations specified above. Reported values are mean ± SEM for three independent experiments that were each fit globally.

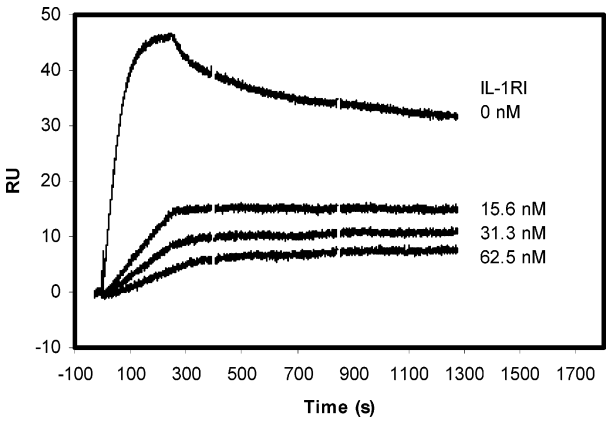

FIGURE 2: Inhibition of human IL-1β binding to Hu007 by IL-1RI. Human IL-1β (3 nM) in the presence of 0, 15.6, 31.3, and 62.5 nM human IL-1RI was injected over the Hu007 surface. The decrease in binding signal (0−240 s) with increasing concentrations of IL-1RI demonstrates that binding of IL-1β by IL-1RI inhibits its binding to Hu007.

important role of electrostatic interactions in binding. The decrease in binding affinity is primarily due to a 12-fold decrease in the k_{on} when the salt concentration is raised from 150 mM to1 M NaCl.

Competitive Binding of Hu007 and IL-1RI to hIL-1β. Because signaling through IL-1RI requires both binding of IL-1β as well as recruitment of IL-1RAcP (*1*−*5*), Hu007 could inhibit activity either by directly blocking the interaction of IL-1β with its receptor or by impeding signaling through perturbation of the ternary complex. We have used Biacore to assess the effect of Hu007 on the IL-1β/IL-1RI interaction. Hu007 was captured on a Biacore chip immobilized with protein A. In the absence of IL-1RI, the maximum binding of IL-1β to Hu007 is achieved at 3 nM IL-1β. Binding of IL-1β to Hu007 is inhibited with increasing concentrations of soluble IL-1RI (Figure 2). If IL-1β was allowed to bind to Hu007 first, injection of 100 nM of IL-1RI does not increase the binding signal, indicating that binding of Hu007 to IL-1β blocks IL-1β binding to its receptor (data not shown). These data together indicate that Hu007 and IL-1RI compete for binding with IL-1β, suggesting that Hu007 neutralizes IL-1β by directly blocking its interaction with the receptor.

Species Cross-Reactivity of Hu007. Binding specificity of Hu007 to IL-1β from different species as well as to human IL-1α and IL-1ra was monitored by surface plasmon resonance (Table 2). In addition to high-affinity binding to human IL-1β, Hu007 binds to cynomolgus, monkey, and rabbit IL-1β with similar affinities. However, Hu007 binds very weakly to rat and mouse IL-1β. The affinity of Hu007 is approximately 6 orders of magnitude lower for mouse than that for human IL-1β. Hu007 does not bind to human IL-1α or human IL-1ra at ligand concentrations up to 300 nM (data not shown).

Table 2: Binding Specificity of Hu007 to IL-1β from Different Species[a]

sample	K_d (pM)	k_{on} (10^7) (M^{-1} s^{-1})	k_{off} (10^{-4}) (s^{-1})
human IL-1β	22 ± 2	2.8 ± 0.4	6.3 ± 0.8
cyno IL-1β	23	2.9	6.5
rabbit IL-1β	17	2.0	3.3
mouse IL-1β	1.2×10^6 [b]	nd	nd
rat IL-1β	1.1×10^5	0.59	6400

[a] Biacore experiments were performed at 25°C in HBS-EP buffer. For IL-1β from human, cynomolgus, and rabbit, the fitting parameters were obtained from a global fit of duplicate runs using six different concentrations of IL-1β ranging from 3 to 0.094 nM in 2-fold serial dilutions. Four independent experiments were performed for human IL-1β to calculate the mean and standard error for the fitting parameters. For mouse and rat IL-1β, binding was performed using six different concentrations ranging from 5000 to 78 nM in 2-fold serial dilutions. [b] nd = not determined. k_{off} was very rapid. K_d was determined by fitting data to a steady-state affinity model.

To identify which residues contribute to species-specific binding and what region of IL-1β is bound by Hu007, we utilized a combination of sequence comparison, site-directed mutagenesis, and H/DXMS analysis.

Effect of Mutations in cIL-1β on Binding of Hu007. Species cross-reactivity data suggest that the epitope recognized by Hu007 must map to a region of the IL-1β that is not completely conserved between the mouse, rat, and human sequences but is conserved among human, cynomolgus, and rabbit IL-1β. Figure 3 depicts an alignment of the mouse, rat, rabbit, cynomolgus, and human IL-1β protein sequences. Positions that are conserved among human, cynomolgus, and rabbit IL-1β but which differ in mouse and rat IL-1β are V3, S5, G22, E51, D76, K77, I106, L110, M130, G140, and F150 (numbering scheme is based on the cynomolgus sequence). Human IL-1β adopts a β-barrel structure as shown by crystallographic analysis (*13*, *12*). Six of these residues (V3, S5, E51, I106, L110, and F150) are located on the open end of the IL-1β barrel. Residues G22, D76, K77, M130, and G140 are located on the closed end of the β barrel on the opposite side. It is likely that only one of these two sides of the IL-1β surface is involved in binding to Hu007.

Using cynomolgus IL-1β as a backbone sequence, a series of experiments were performed to assess the effect of converting selected residues to those present in mouse IL-1β. To simplify purification of multiple forms of cIL-1β, a C-terminal 6× His tag form of IL-1β was used. As shown in Table 3, addition of the 6× His tag increased the K_d from 23 pM (Table 2) to 40 pM, an approximately 2-fold decrease in binding affinity. This was judged to be an acceptable decrease in affinity; therefore, subsequent studies were performed with 6× His-tagged proteins.

Kinetic parameters for binding to Hu007 were evaluated for the following mutant forms of cIL-1β: G22D, E51P, L110V, and F150S. The following combinations of mutant forms were also tested: V3I/S5Q, D76G/K77T, and V3I/S5Q/F150S. The G140Δ, referring to the G140 deletion mutant, was also made; however, it failed to express in *E. coli* and was not studied further.

FIGURE 3: Sequence alignment of human, cynomolgus, rabbit, rat, and mouse IL-1β. Sequences of the mature forms of IL-1β are shown. Residues that are identical in human (h), cynomolgus (c), and rabbit IL-1β (rb) and differ in mouse (m) and rat IL-1β (r) are shaded. Mutant forms of cynomolgus and mouse IL-1β were expressed with a C-terminal poly-histidine tag for ease of purification. The C-terminal tag is shown in bold, underlined type.

Table 3: Binding Affinity and Kinetics of cIL-1β Wild Type and Analogues Determined by Biacore[a]

analogue	K_d (pM)	fold increase in K_d	k_{on} (10^7) (M^{-1} s^{-1})	k_{off} (10^{-3}) (s^{-1})
cIL-1β (6× His tagged)				
wild type	40 ± 3	1	3 ± 1	1.3 ± 0.7
E51P	32.6	0.8	2.8	0. 9
G22D	47.9	1.2	2.3	1.1
L110V	115	2.9	2.7	2.4
V3I/S5Q	151	3.8	1.7	2.5
F150S	4720	118	0.6	25.8
V3I/S5Q/F150S	47 300[b]	1183		
mouse IL-1β (6× His tagged)				
wild type	1.2×10^6 [b]	1	nd	nd
I3V/Q5S/S150F	3000	0.0025	1.4	42.4

[a] Biacore experiments were performed at 25°C in HBS-EP buffer. [b] nd = not determined. k_{off} was very rapid. K_d was determined by fitting data to a steady-state affinity model.

The single mutations E51P and G22D had no effect on binding (Table 3). The D76G/K77T combination mutation did not alter binding (data not shown). In contrast, residues on the open end of the β barrel are involved in binding to Hu007. The mutation V3I/S5Q led to an approximately 4-fold decrease in affinity. Mutation L110V decreased the affinity by about 3-fold. The F150S mutation substantially increased the k_{off} for the complex and led to a 100-fold decrease in binding affinity, suggesting a significant role of hydrophobic interactions in stabilizing the antibody/antigen complex. As can be seen from Table 3, the triple mutation V3I/S5Q/F150S decreased affinity by about 3 orders of magnitude and led to a very rapid dissociation rate. These data suggest that residues at positions 3, 5, and 150 form critical components of the Hu007-binding epitope and that these residues have a synergistic effect on binding. To further confirm the importance of these residues in antibody binding, residues 3, 5, and 150 in mouse IL-1β were mutated to the residues common to human, cynomolgus, and rabbit (I3V/Q5S/S150F). This triple-mutant binds Hu007 with a K_d of 3.7 nM, an improvement of approximately 3 orders of magnitude when compared to a K_d of 1.2 μM for wild-type mouse IL-1β.

The mutations on IL-1β could impact Hu007 binding by directly altering interactions with Hu007 or by changing the structure of IL-1β, consequently affecting binding. To determine whether the mutations impact the structure of IL-1β, far- and near-UV CD spectroscopy was used to compare the secondary and tertiary structure of IL-1β analogues to the native structure. The CD spectra of all IL-1β analogues were similar (data not shown), indicating that the mutations do not disrupt the secondary and tertiary structure of IL-1β. These data suggest that V3, S5, and F150 are likely to be in direct contact with Hu007.

Identification of Binding Regions of IL-1β by Hu007 Using H/DXMS Analysis. In addition to nonconserved residues, conserved residues could also participate in binding. To map out the complete binding interface, we employed H/DXMS to identify regions of human IL-1β that are protected from exchange with deuterated water (D_2O) because of the binding to Hu007. The exchange rate of amide hydrogen in protein/protein complexes is highly dependent on whether the amide groups participate in binding. Free IL-1β or the IL-1β/Hu007 complex in water was mixed with D_2O to allow exchange of amide protons by deuterium. Those backbone amide groups that participate in protein binding are protected from exchange and remain protonated. These regions were then identified by peptic proteolysis, coupled with LC and electrospray ionization mass spectrometry.

The first step in this procedure is to assign peptic peptides for IL-1β. Peptic peptides identified for free IL-1β covered the entire sequence. One peptide (9−35) identified in free IL-1β was not found or was difficult to assign in the Hu007/IL-1β complex. This was attributable, in part, to the existence of large mass signals from the digested antibody that coeluted with the 9−35 peptide.

When Hu007 forms a complex with IL-1β, the binding region (epitope) of IL-1β is protected from the solvent. This leads to slower amide hydrogen exchange rates when compared to those of IL-1β alone. The peptides protected from exchange because of complex formation should differ in the extent of exchange compared to the corresponding peptides in IL-1β alone. An example of mass spectra for two peptides is shown in Figure 4. Table 4 lists mass differences obtained by H/DXMS for the peptic peptides between the free and complexed IL-1β. Upon binding of Hu007, the IL-1β peptides 1−10, 2−8, 46/47−71, and 146−149 show significant mass differences after the deuterium exchange. The peptide 150−153 has a small but statistically significant mass difference. The mass difference for most

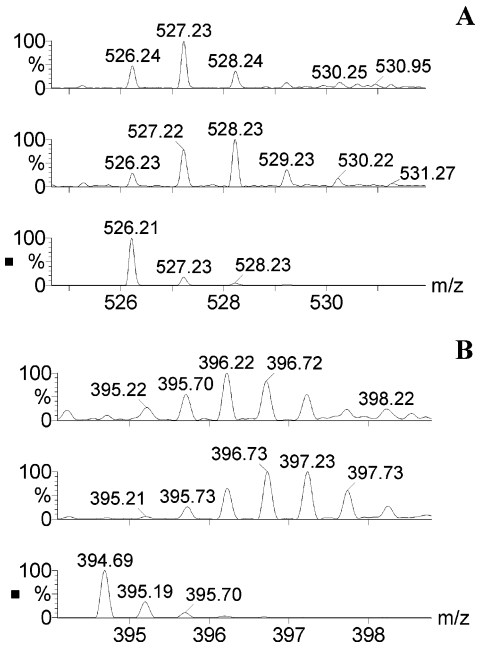

FIGURE 4: Mass spectra of the peptic peptides of IL-1β: (A) 2−8; (B) 146−149. The top and middle levels of each panel are the mass spectra of IL-1β peptides with or without Hu007 after H/D exchange, respectively. The bottom level is the mass spectrum of the same peptide without H/D exchange.

Table 4: Difference in Mass of IL-1β Peptides Obtained by LC/MS Analysis for IL-1β and IL-1β/Hu007 after H/D Exchange

peptide	Δmass (Da)[a] (average $\pm$ SD)
1−10	-1.1 ± 0.3
2−8	-0.7 ± 0.3
39−42	-0.1 ± 0.3
46−71	-0.4 ± 0.1
47−71	-0.6 ± 0.2
72−82	0.0 ± 0.2
83−112	-0.2 ± 0.3
113−120	0.0 ± 0.2
121−133	-0.2 ± 0.1
134−145	-0.1 ± 0.1
146−149	-0.5 ± 0.2
150−153	-0.2 ± 0.01

[a] ΔMass was calculated by (average mass of IL-1β/Hu007 complex) − (average mass of IL-1β only) for the same peptic peptide. SD denotes the standard deviation of measurements calculated from three or more independent experiments.

of the peptides is less than 1 Da. During the peptic digest and LC/MS analysis, back exchange could occur at up to 50% for very small peptides (on the basis of control experiments, data not shown). Thus, if the back exchange could be completely prevented, the mass difference detected would be 1−2 Da for these peptides. Except for Pro and N-terminal residues, each amino acid residue has a single amide hydrogen; therefore, after deuterium exchange, the peptide or protein mass increases 1 Da per amide hydrogen. Hence, a 1 or 2 Da difference means that one or two amino acid residues in those peptides were protected from exchange by the antibody; i.e., they were involved in binding (belong to the epitope) or that they were in contact with non-CDR regions of the antibody. In the case of peptide 150−153, the amide hydrogen of F150 is an N-terminal amide, which, as noted above, has a much higher exchange rate than other amide hydrogens. Although all of the data are not consistent

FIGURE 5: Ribbon representation of the IL-1β structure (*12*). Peptides that are protected from exchange upon Hu007 binding (2−8, 47−71, and 146−153) are shown in yellow. CPK representation of the side chains of three residues important for binding to Hu007 is shown in cyan. Side chains of other residues that do not have significant impact on binding upon mutation are represented as ball-and-stick models.

with the structure of the epitope, e.g., N-terminal exchange of F150, this inconsistent data can be explained in a manner that does not detract from the assignment of the Hu007 epitope. Figure 5 highlights these peptides in the 3D structural model of IL-1β (*12*, *13*). The data indicate that the IL-1β epitope for Hu007 is conformational and could consist of at least one or two amino acid residues from each peptide 2−8, 47−71, and 146−153.

DISCUSSION

In this study, we have employed surface plasmon resonance technology to measure the binding kinetics, affinity, and specificity of humanized antibody Hu007 with IL-1β. The interaction is shown to be highly specific and strongly dependent on the salt concentration. Similar salt-dependent binding properties have been observed for a number of protein/protein interactions and are attributed to an important role of electrostatic interactions in facilitating complex formation via electrostatic steering (*18*−*23*). Electrostatic surface potentials of Hu007 and IL-1β were calculated using GRASP. The electrostatic modeling of IL-1β was based on a structure from the PDB (1ITB), and the electrostic modeling of Hu007 was based on a homology model of the variable domain (*24*). As shown in Figure 6, the CDR-binding regions of Hu007 are largely negatively charged. On the other hand, positively charged patches were observed on the binding surface of IL-1β. The favorable charge complementarity between Hu007 and IL-1β could facilitate their association. Although the three key residues (V3, S5,

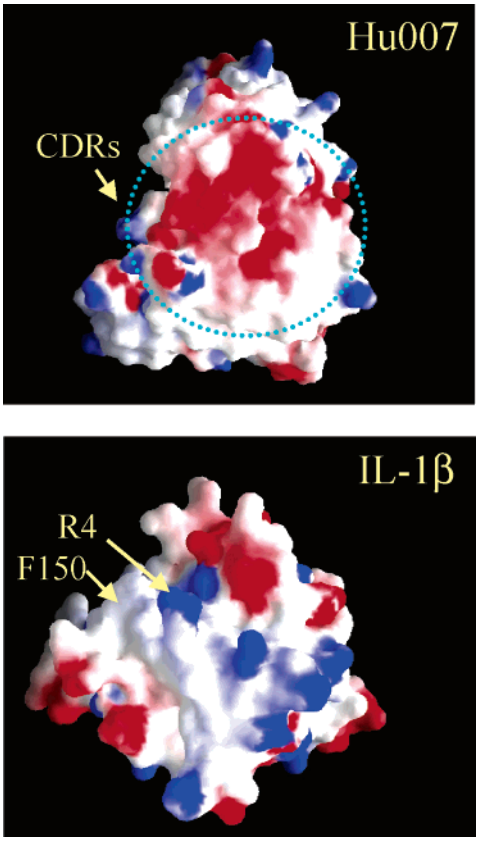

FIGURE 6: Electrostatic surface potential of Hu007 and human IL-1β calculated using GRASP (*24*) at a salt concentration of 0.15 M NaCl. The Hu007 variable region structure was derived from homology modeling. The IL-1β (1ITB) structure was RCSB−PDB. The binding region (circled CDRs) of Hu007 is negatively charged (red). A patch of positive-charged surface (blue) was observed for human IL-1β.

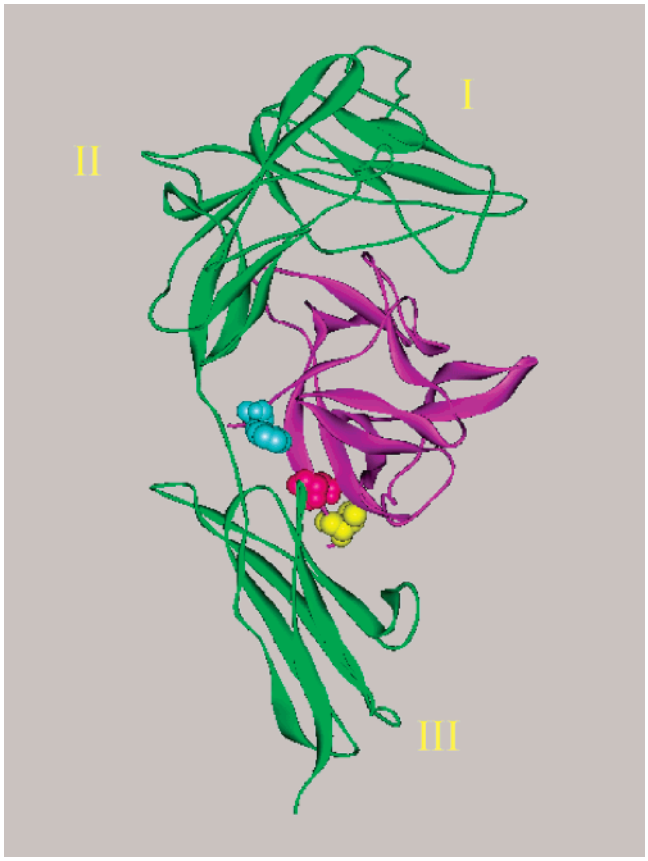

FIGURE 7: Ribbon representation of the structure for the human IL-1β and IL-1RI complex (*28*). Receptor domain III interacts with the open end of the IL-1β barrel where the N and C termini of the protein reside. The side chains of V3, S5, and F150 identified as critical for binding to Hu007 are shown in yellow, red, and cyan, respectively, located at the interface between IL-1β and its receptor.

and F150), identified to be critical for species specificity, are not charged, other residues that are conserved among human, cynomolgus, rabbit, and mouse IL-1β may also form part of the Hu007 epitope. For example, the conserved Arg4 could also play an important role in the interaction between IL-1β and Hu007. It should be noted that the CDRs of Hu007 contain several aspartic acid residues; thus, electrostatic interaction between R4 and Asp residues in Hu007 could contribute to the observed favorable electrostatic interactions in binding as well.

Extensive site-directed mutagenesis studies have been carried out previously to identify residues on IL-1β that are critical for binding to its receptor (*25*− *27*). These studies suggested two main sites on the surface of IL-1β, with one site (site A) located on the closed-end side of the barrel and the other site (site B) located at the open-end side of the barrel. The N and C termini are located at the open end of the barrel and are involved in interacting with receptor domain III (Figure 7, *28*). For example, studies using site-directed mutagenesis and chemical modification have shown that Arg4 is critical for IL-1β binding to its receptor (*29*, *25*). The three residues in IL-1β critical for high-affinity binding by Hu007 are located in this region. Consequently, binding of Hu007 to this region of IL-1β can directly block IL-1β interaction with its receptor.

To further define the binding regions on IL-1β, we utilize H/DXMS analysis. This technique has been widely used to determine protein structure, stability, dynamics, ligand-binding affinity, and map protein/protein-binding interfaces (*30*−*37*). The three residues that are critical for binding and species specificity (V3, S5, and F150) are located in two of the peptides identified by H/DXMS. Although another fairly large peptide (47−71) was also identified by H/DXMS, the residues in this region of IL-1β from different species are highly conserved, differing only in position 51 (Glu in human, cynomolgus, and rabbit IL-1β; Pro in mouse IL-1β; and Thr in rat IL-1β). To address the involvement of E51, this site was mutated to a proline in cIL-1β and showed no impact on binding affinity to Hu007, suggesting that this residue is not directly involved in binding. Nonetheless, we could not rule out the possibility that conserved residues in this region may also be involved in binding and/or that this region is perturbed structurally because of the binding of Hu007.

Two other sites, L110 and M130, were also considered as possibly participating in the binding domain. In regard to residue M130, this site was not mutated because it is on the closed-end side of the barrel and could not contact the antibody. In regard to residue L110, although this residue is near the IL-1β−Hu007 interface and did affect binding, we feel it is unlikely to be a critical contact residue, because H/DXMS analysis did not show any protection by the antibody. It is likely that the effect on binding is due to steric effects of the mutation.

This work illustrates the value of taking multiple approaches for epitope mapping. For a discontinuous conformational epitope like that of Hu007, attempting to identify a peptide that the antibody binds would be difficult or impossible. Without the binding data and sequence comparisons, the hydrogen/deuterium exchange could have led to the conclusion that peptide 47−71 formed a critical part of the epitope. Using only sequence comparisons and mutagenesis to determine binding would have missed the potential interactions of Hu007 and 47−71. Thus, a strategy utilizing orthogonal appoaches in this work can offer a more complete picture of antibody/antigen interactions than a single method. A detailed definition of IL-1β epitopes will aid in the understanding of IL-1β function and the mechanism of molecules that block IL-1β function. The knowledge gained could assist in designing more effective antibody therapeutics to treat various inflammatory diseases in which IL-1β is involved.

ACKNOWLEDGMENT

We are grateful to S. Bright for his help with Biacore experiments and M. Johnson for development of the triple mutant. We would also like to thank Dr. R. Darling for critical reading of the manuscript and helpful discussions.

REFERENCES

1. O'Neill, L. A., and Greene, C. (1998) Signal transduction pathways activated by the IL-1 receptor family: Ancient signaling machinery in mammals, insects, and plants, *J. Leukocyte Biol. 63*, 650−657.
2. Auron, P. E. (1998) The Interleukin 1 (IL-1) receptor: Ligand interactions and signal transduction, *Cytokine Growth Factor Rev. 9*, 221−237.
3. Sims, J. E., Giri, J. G., and Dower, S. K. (1994) The two interleukin-1 receptors play different roles in IL-1 actions, *Clin. Immunol. Immunopathol. 72*, 9−14.
4. Jensen, L. E., Muzio, M., Mantovani, A., and Whitehead, A. S. (2000) IL-1 signaling cascade in liver cells and the involvement of a soluble form of the IL-1 receptor accessory protein, *J. Immunol. 164*, 5277−5286.
5. Lang, D., Knop, J., Wesche, H., Raffetseder, U., Kurrle, R., Boraschi, D., and Martin, M. U. (1998) The type II IL-1 receptor interacts with the IL-1 receptor accessory protein: A novel mechanism of regulation of IL-1 responsiveness, *J. Immunol. 161*, 6871−6877.
6. Colotta, F., Dower, S. K., Sims, J. E., and Mantovani, A. (1994) The type II "decoy" receptor: A novel regulatory pathway for interleukin 1, *Immunol. Today 15*, 562−566.
7. Colotta, F., Re, F., Muzio, M., Bertini, R., Polentarutti, N., Sironi, M., Giri, J. G., Dower, S. K., Sims, J. E., and Mantovani, A. (1993) Interleukin-1 type II receptor: A decoy target for IL-1 that is regulated by IL-4, *Science 261*, 472−475.
8. Arend, W. P., Malyak, M., Smith, M. F., Jr., Whisenand, T. D., Slack, J. L., Sims, J. E., Giri, J. G., and Dower, S. K. (1994) Binding of IL-1α, IL-1β, and IL-1 receptor antagonist by soluble IL-1 receptors and levels of soluble IL-1 receptors in synovial fluids, *J. Immunol. 153*, 4766−4774.
9. Dower, S. K., Fanslow, W., Jacobs, C., Waugh, S., Sims, J. E., and Widmer, M. B. (1994) Interleukin-I antagonists, *Ther. Immunol. 1*, 113−122.
10. Bresnihan, B. (2002) Anakinra as a new therapeutic option in rheumatoid arthritis: Clinical results and perspectives, *Clin. Exp. Rheumatol. 20*, S32−S34.
11. Zwerina, J., Hayer, S., Tohidast-Akrad, M., Bergmeister, H., Redlich, K., Feige, U., Dunstan, C., Kollias, G., Steiner, G., Smolen, J., and Schett, G. (2004) Single and combined inhibition of tumor necrosis factor, interleukin-1, and RANKL pathways in tumor necrosis factor-induced arthritis: Effects on synovial inflammation, bone erosion, and cartilage destruction, *Arthritis Rheum. 50*, 277−290.
12. Finzel, B. C., Clancy, L. L., Holland, D. R., Muchmore, S. W., Watenpaugh, K. D., and Einspahr, H. M. (1989) Crystal structure of recombinant human interleukin-1β at 2.0 Å resolution, *J. Mol. Biol. 209*, 779−791.
13. Priestle, J. P., Schar, H. P., and Grutter, M. G. (1988) Crystal structure of the cytokine interleukin-1β, *EMBO J. 7*, 339−343.
14. Vigers, G. P., Caffes, P., Evans, R. J., Thompson, R. C., Eisenberg, S. P., and Brandhuber, B. J. (1994) X-ray structure of interleukin-1 receptor antagonist at 2.0 Å resolution, *J. Biol. Chem. 269*, 12874−12879.
15. Schreuder, H. A., Rondeau, J. M., Tardif, C., Soffientini, A., Sarubbi, E., Akeson, A., Bowlin, T. L., Yanofsky, S., and Barrett, R. W. (1995) Refined crystal structure of the interleukin-1 receptor antagonist. Presence of a disulfide link and a *cis*-proline, *Eur. J. Biochem. 227*, 838−847.
16. Stockman, B. J., Scahill, T. A., Strakalaitis, N. A., Brunner, D. P., Yem, A. W., and Deibel, M. R., Jr. (1994) Solution structure of human interleukin-1 receptor antagonist protein, *FEBS Lett. 349*, 79−83.
17. Graves, B. J., Hatada, M. H., Hendrickson, W. A., Miller, J. K., Madison, V. S., and Satow, Y. (1990) Structure of interleukin 1α at 2.7 Å resolution, *Biochemistry 29*, 2679−2684.
18. Darling, R. J., Kuchibhotla, U., Glaesner, W., Micanovic, R., Witcher, D. R., and Beals, J. M. (2002) Glycosylation of erythropoietin affects receptor binding kinetics: Role of electrostatic interactions, *Biochemistry 41*, 14524−14531.
19. Karshikov, A., Bode, W., Tulinsky, A., and Stone, S. R. (1992) Electrostatic interactions in the association of proteins: An analysis of the thrombin−hirudin complex, *Protein Sci. 1*, 727−735.
20. Selzer, T., and Schreiber, G. (1999) Predicting the rate enhancement of protein complex formation from the electrostatic energy of interaction, *J. Mol. Biol. 287*, 409−419.
21. Selzer, T., Albeck, S., and Schreiber, G. (2000) Rational design of faster associating and tighter binding protein complexes, *Nat. Struct. Biol. 7*, 537−541.
22. Selzer, T., and Schreiber, G. (2001) New insights into the mechanism of protein−protein association, *Proteins 45*, 190−198.
23. Wendt, H., Leder, L., Harma, H., Jelesarov, I., Baici, A., and Bosshard, H. R. (1997) Very rapid, ionic strength-dependent association and folding of a heterodimeric leucine zipper, *Biochemistry 36*, 204−213.
24. Nicholls, A., Sharp, K. A., and Honig, B. (1991) Protein folding and association: Insights from the interfacial and thermodynamic properties of hydrocarbons, *Proteins 11*, 281−296.
25. Evans, R. J., Bray, J., Childs, J. D., Vigers, G. P., Brandhuber, B. J., Skalicky, J. J., Thompson, R. C., and Eisenberg, S. P. (1995) Mapping receptor binding sites in interleukin (IL)-1 receptor antagonist and IL-1β by site-directed mutagenesis. Identification of a single site in IL-1ra and two sites in IL-1β, *J. Biol. Chem. 270*, 11477−11483.
26. Grutter, M. G., van Oostrum, J., Priestle, J. P., Edelmann, E., Joss, U., Feige, U., Vosbeck, K., and Schmitz, A. (1994) A mutational analysis of receptor binding sites of interleukin-1β: Differences in binding of human interleukin-1β muteins to human and mouse receptors, *Protein Eng. 7*, 663−671.
27. Labriola-Tompkins, E., Chandran, C., Kaffka, K. L., Biondi, D., Graves, B. J., Hatada, M., Madison, V. S., Karas, J., Kilian, P. L., and Ju, G. (1991) Identification of the discontinuous binding site in human interleukin 1β for the type I interleukin 1 receptor, *Proc. Natl. Acad. Sci. U.S.A. 88*, 11182−11186.
28. Vigers, G. P., Anderson, L. J., Caffes, P., and Brandhuber, B. J. (1997) Crystal structure of the type-I interleukin-1 receptor complexed with interleukin-1β, *Nature 386*, 190−194.
29. Nanduri, V. B., Hulmes, J. D., Pan, Y. C., Kilian, P. L., and Stern, A. S. (1991) The role of arginine residues in interleukin 1 receptor binding, *Biochim. Biophys. Acta 1118*, 25−35.
30. Hoofnagle, A. N., Resing, K. A., and Ahn, N. G. (2004) Practical methods for deuterium exchange/mass spectrometry, *Methods Mol. Biol. 250*, 283−298.
31. Hoofnagle, A. N., Resing, K. A., and Ahn, N. G. (2003) Protein analysis by hydrogen exchange mass spectrometry, *Annu. Rev. Biophys. Biomol. Struct. 32*, 1−25.
32. Baerga-Ortiz, A., Hughes, C. A., Mandell, J. G., and Komives, E. A. (2002) Epitope mapping of a monoclonal antibody against human thrombin by H/D-exchange mass spectrometry reveals

selection of a diverse sequence in a highly conserved protein, *Protein Sci. 11*, 1300−1308.
33. Ehring, H. (1999) Hydrogen exchange/electrospray ionization mass spectrometry studies of structural features of proteins and protein/protein interactions, *Anal. Biochem. 267*, 252−259.
34. Hamuro, Y., Coales, S. J., Southern, M. R., Nemeth-Cawley, J. F., Stranz, D. D., and Griffin, P. R. (2003) Rapid analysis of protein structure and dynamics by hydrogen/deuterium exchange mass spectrometry, *J. Biomol. Technol. 14*, 171−182.
35. Woods, V. L., Jr., and Hamuro, Y. (2001) High resolution, high-throughput amide deuterium exchange-mass spectrometry (DXMS) determination of protein binding site structure and dynamics: Utility in pharmaceutical design, *J. Cell. Biochem. Suppl.* 89−98.
36. Zhu, M. M., Rempel, D. L., and Gross, M. L. (2004) Modeling data from titration, amide H/D exchange, and mass spectrometry to obtain protein−ligand binding constants, *J. Am. Soc. Mass Spectrom. 15*, 388−397.
37. Engen, J. R., and Smith, D. L. (2000) Investigating the higher order structure of proteins. Hydrogen exchange, proteolytic fragmentation, and mass spectrometry, *Methods Mol. Biol. 146*, 95−112.

BI0505464